AGU PUBLICATIONS

Geophysical Research Letters

RESEARCH LETTER
10.1002/2016GL071733

Key Points:
- Elevated atmospheric CO_2 influences climate through both radiative and physiological effects
- Warming caused by CO_2 radiative forcing effect has an overall little impact on global GPP
- Climate change caused by CO_2 physiological effect significantly weakens CO_2 fertilization mainly by reducing precipitation

Supporting Information:
- Supporting Information S1

Correspondence to:
Q. Zhuang,
qzhuang@purdue.edu

Citation:
Zhu, P., Q. Zhuang, P. Ciais, L. Welp, W. Li, and Q. Xin (2017), Elevated atmospheric CO_2 negatively impacts photosynthesis through radiative forcing and physiology-mediated climate feedback, *Geophys. Res. Lett.*, *44*, doi:10.1002/2016GL071733.

Received 28 OCT 2016
Accepted 13 FEB 2017
Accepted article online 16 FEB 2017

Elevated atmospheric CO_2 negatively impacts photosynthesis through radiative forcing and physiology-mediated climate feedback

Peng Zhu[1], Qianlai Zhuang[1,2], Philippe Ciais[3], Lisa Welp[1], Wenyu Li[4], and Qinchuan Xin[5]

[1]Department of Earth, Atmospheric, and Planetary Sciences, Purdue University, West Lafayette, Indiana, USA, [2]Department of Agronomy, Purdue University, West Lafayette, Indiana, USA, [3]Laboratoire des Sciences du Climat et de l'Environnement, CEA, CNRS, UVSQ Gif-sur-Yvette, France, [4]Ministry of Education Key Laboratory for Earth System Modeling, Tsinghua University, Beijing, China, [5]Department of Geography and Planning, Sun Yat-Sen University, Guangzhou, China

Abstract Increasing atmospheric CO_2 affects photosynthesis involving directly increasing leaf carboxylation rates, stomatal closure, and climatic effects. The direct effects are generally thought to be positive leading to increased photosynthesis, while its climatic effects can be regionally positive or negative. These effects are usually considered to be independent from each other, but they are in fact coupled through interactions between land surface exchanges of gases and heat and the physical climate system. In particular, stomatal closure reduces evapotranspiration and increases sensible heat emissions from ecosystems, leading to decreased atmospheric moisture and precipitation and local warming. We use a coupled earth system model to attribute the influence of the increase in CO_2 on gross primary productivity (GPP) during the period of 1930–2011. In our model, CO_2 radiative effects cause climate change that has only a negligible effect on global GPP (a reduction of $0.9 \pm 2\%$ during the last 80 years) because of opposite responses between tropical and northern biomes. On the other hand, CO_2 physiological effects on GPP are both positive, by increased carboxylation rates and water use efficiency ($7.1 \pm 0.48\%$ increase), and negative, by vegetation-climate feedback reducing precipitation, as a consequence of decreased transpiration and increased sensible heat in areas without water limitation ($2.7 \pm 1.76\%$ reduction).When considering the coupled atmosphere-vegetation system, negative climate feedback on photosynthesis and plant growth due to the current level of CO_2 opposes 29–38% of the gains from direct fertilization effects.

1. Introduction

Gross primary productivity (GPP) plays a crucial role in driving the land carbon cycle. Process-based and data-driven models have been used to evaluate how global GPP responds to climate change and rising CO_2 concentrations [*Beer et al.*, 2010; *Jung et al.*, 2011; *Piao et al.*, 2013]. Models and field experiments agree on the fact that elevated CO_2 increases carboxylation rates and GPP (hereafter fertilization effect) in absence of nutrient limitations and decreases leaf-scale stomatal conductance [*Medlyn et al.*, 2015]. The radiative forcing of elevated CO_2 (eCO_2) also causes climate change, which can increase or reduce GPP depending on regional temperature and water limitations, with water limitations being today prominent over most of ecosystems [*Beer et al.*, 2010]. Therefore, there are large uncertainties about the magnitude and regional patterns of the net GPP response to the joint perturbation of eCO_2 concentration and climate change [*Beer et al.*, 2010]. Most studies of GPP trends with process-based land carbon models have been conducted by using so-called off-line simulations where atmospheric forcing conditions are imposed to an ecosystem model, but there is no feedback from the land surface to the atmosphere [*Piao et al.*, 2013; *Beer et al.*, 2010]. Coupled climate-carbon cycle models include both impacts of CO_2 through climate change and vegetation fertilization, but previous simulations did not fully separate the two mechanisms [*Friedlingstein et al.*, 2006; *Arora et al.*, 2013; *Matthews et al.*, 2007]. In a coupled climate-carbon models, climate change affects GPP differently across regions and time of the year, depending upon local temperature or water limitations [*Matthews et al.*, 2007; *Cox et al.*, 2000]. In addition, vegetation-climate feedback occur when plants close their stomates and decreased transpiration under elevated CO_2. This antitranspirant effect of eCO_2 leads to more soil moisture being available for plants in the dry season and changes the partition of net radiation between

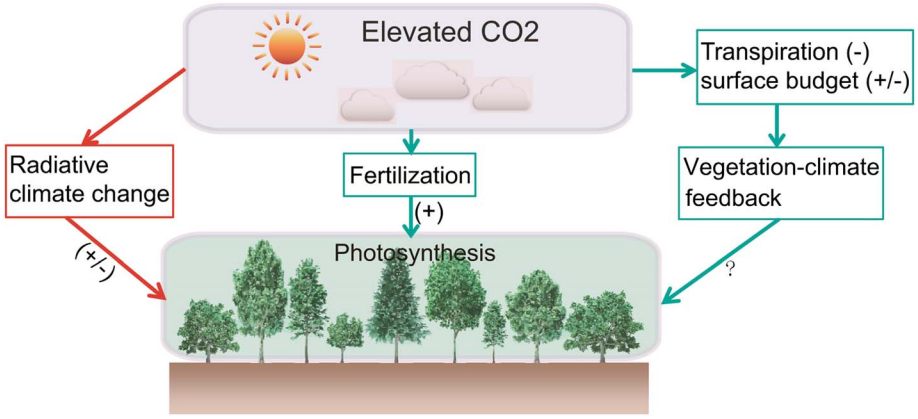

Figure 1. Schematic diagram of CO_2's three pathway influence on terrestrial GPP. The rising atmospheric CO_2 concentration will facilitate plant uptake of CO_2 through photosynthesis (fertilization effect). CO_2 also influences plant photosynthesis indirectly through its climate forcing effect. Its impact on climate through trapping longwave radiation (radiative climate change) can increase Earth's mean surface temperature and thus influence plant photosynthesis. The response of plants to rising CO_2 can cause an increase in foliage cover and decreases leaf transpiration by reducing stomatal conductance per unit leaf area, which also impact climate system (vegetation-climate feedback) and thus influence plant photosynthesis indirectly.

latent heat (evapotranspiration) and sensible heat. Increases in vegetation cover and leaf area index due to CO_2 fertilization can, however, offset the effect of leaf-level stomatal closure by increasing the surface of leaves available for transpiration [*Ukkola et al.*, 2015; *Donohue et al.*, 2013].

Previous research on carbon-climate feedback under eCO_2 mainly focused on the eCO_2-fertilization (a negative feedback on climate change through increased carbon sinks caused by higher GPP) and on eCO_2-induced climate change. Vegetation-climate feedback under eCO_2 have been shown to decrease atmospheric humidity [*Cao et al.*, 2010] and precipitation [*Andrews et al.*, 2011; *Boucher et al.*, 2009], which warms land surface temperature and in turn impacts GPP. But the effect of climate change from eCO_2 through vegetation-climate feedback on GPP has not been separated from the CO_2-fertilization effect in previous studies. Here we use the terms eCO_2-VCF to denote climate change caused by vegetation-climate feedback under eCO_2 and eCO_2-FERT for the CO2 fertilization effects on GPP. The diagram in Figure 1 presents the three mechanisms by which eCO_2 influences GPP and ecosystem carbon cycling. This study aims to isolate these mechanisms for their impact on terrestrial GPP in a series of factorial experiments with the Community Earth System Model-Biogeochemistry (CESM-BGC) Earth System model integrated from 1850 to 2011.

2. Methods

The CESM1.2.2-BGC Earth System model is used in this study, its land model being CLM4.5CN. To distinguish the effects of eCO_2-FERT and eCO_2-VCF in determining changes on terrestrial GPP, we performed 162 year (1850–2011) simulations at 2.5° × 1.9° spatial resolution with six scenarios as follows: (1) A control simulation (CTR), in which the coupled atmosphere land carbon system is forced by the preindustrial CO_2 concentration of 285 ppm; (2) a CO_2 radiative climate change simulation (eCO_2-RAD), in which GPP is only influenced by CO_2 radiative effects; to this end, the atmosphere was forced by transient (1850–2011) CO_2 concentration, while GPP was calculated by using the preindustrial CO_2 concentration; (3) an eCO_2-FERT + VCF simulation, in which GPP responds to both CO_2 fertilization and climate change from vegetation-climate feedback; to do so, the land model of CESM1.2.2-BGC was forced by a transient CO_2 concentration, while the atmospheric model was forced by the preindustrial CO_2 concentration; (4) an off-line control simulation (OCTR) in which the CTR climate variables were used to drive the CLM4.5CN land model in an off-line mode, with the preindustrial CO_2 concentration of 285 ppm; (5) an off-line CO_2 fertilization simulation (eCO_2-FERT) with transient CO_2 and CTR climate variables; and (6) a coupled simulation (ALL) with both land and atmosphere driven by transient CO_2 (Table S1 in the supporting information). All experiments were configured with the same initial

conditions, namely, a 500 years to approach equilibrium. Solar forcing, ozone concentrations, non-CO_2 greenhouse gases, and historical land use forcing is transient in all our simulations and were kept the same among the six experiments. Analysis was conducted for the years after 1930 in each simulation, thus disregarding the first 80 years after spin-up.

Annual mean GPP difference (ΔGPP) between eCO_2-RAD and CTR attributes the effect of CO_2-induced radiative climate change. The ΔGPP between eCO_2-FERT and OCTR attributes the effect of fertilization alone, in absence of eCO_2-VCF. The ΔGPP between eCO_2 VCF + FERT and eCO_2-FERT-OCTR attributes the effect of e-CO_2-VCF alone. The precipitation ΔPrec and surface air temperature ΔTsa differences during the growing season were used to assess the impact of climate change on ΔGPP. The growing season is here defined for simplicity as the months with GPP larger than 5% of the annual maximum GPP [*Melaas et al*., 2013]. The $\Delta Prec_{rad}$ and ΔTsa_{rad} were derived through the corresponding variable differences between RAD and CTR. In eCO_2-VCF + FERT, GPP responds to both fertilization and eCO_2-VCF, while climate is only influenced by eCO_2-VCF, so $\Delta Prec_{VCF}$ and ΔTsa_{VCF} can be derived based on corresponding variable differences between VCF + FERT and CTR (Table S2).

The equations governing leaf carbon and water flux in the land model (CLM4.5CN) use the Ball-Berry stomatal conductance model [*Ball et al*., 1987; *Collatz et al*., 1991] and the Farquhar photosynthesis model [*Farquhar et al*., 1980]. The Ball-Berry model scales stomatal conductance (g_s) with relative humidity (RH) and the ratio of assimilation (A_n) to atmospheric CO_2 concentration (C_s), such that $g_s = g_0 + g_1 RH A_n/C_s$. The latitudinal pattern of annual mean evapotranspiration (ET) and GPP in the period of 1982–2011 in experiment "ALL" was compared to the data-driven product from *Jung et al*., 2011 and shows quite similar patterns (Figure S1 in the supporting information). A key metrics linking the water with carbon flux, is the intrinsic water use efficiency (iWUE) defined as A_n/g_s, was diagnosed in the simulation ALL. The response of iWUE to rising CO_2 is positive and similar in magnitude to the one deduced from tree ring isotopes: for boreal forest the largest increase in iWUE (31%) and an increase in temperate and tropical forest iWUE of 26% and 19% per 100 ppm CO_2, respectively (Figure S2), comparable with tree ring isotope-based estimates [*Frank et al*., 2015; *van der Sleen et al*., 2015].

To test the robustness of our results with respect to the choice of a specific earth system model, we also used the output of the Institut Pierre-Simon Laplace Coupled Model 5A Low Resolution (IPSL-CM5A-LR) earth system model from the Coupled Model Intercomparison Project Phase 5 (CMIP5) over 1850–2005 which performed the set of simulations needed to separate eCO_2-RAD and eCO_2-FERT + VCF on GPP. The eCO_2-FERT contribution in IPSL-CM5A-LR was approximated by the results of *Piao et al*. [2013] using an off-line run of the same land carbon model. Model outputs from IPSL-CM5A-LR in CMIP5 are from the "historical," "esmFixClim2," and "esmFdbk2" experiments over 1850–2005 (Table S2) [see *Taylor et al*., 2012]. The experiment historical is forced with all conditions changed (consistent with observations). Experiment esmFixClim2 is forced with changing conditions, except that the radiation code uses preindustrial CO_2 concentration. The experiment esmFdbk2 was forced with changing conditions except for the land component being prescribed with preindustrial CO_2. In summary, the difference between historical and esmFixClim2 attributes eCO_2-RAD effects, and the difference between historical and esmFdbk2 attributes eCO_2-FERT + VCF effects.

3. Results

The first 80 years of simulation results were disregarded as spin-up, and model outputs were analyzed from 1930 to 2011. First, spatially coherent positive trends of GPP are found from the fertilization effect (ΔGPP_{FERT}), with tropical regions showing the largest positive response; these regions have little climate limitation of GPP and are weakly limited by nitrogen in our model (Figure 2a). Second, CO_2 radiative climate change causes regionally different GPP trends (ΔGPP_{RAD}), namely, a positive effect in the northern latitudes and a negative one in tropical and subtropical regions (Figure 2b). In the southern hemisphere and the tropics (60°S to 30°N), ΔGPP_{RAD} shows nonsignificant negative trends, but temperate (30°N–60°N) and boreal areas (60°N–90°N) show significantly positive ΔGPP_{RAD} ($p < 0.01$). Third, changes of GPP due to vegetation-climate feedback (ΔGPP_{VCF}) are mainly negative, except in the northern high latitudes; the latitudinal band between 60°S and 30°S shows the largest negative ΔGPP_{VCF} changes (Figure 2c).

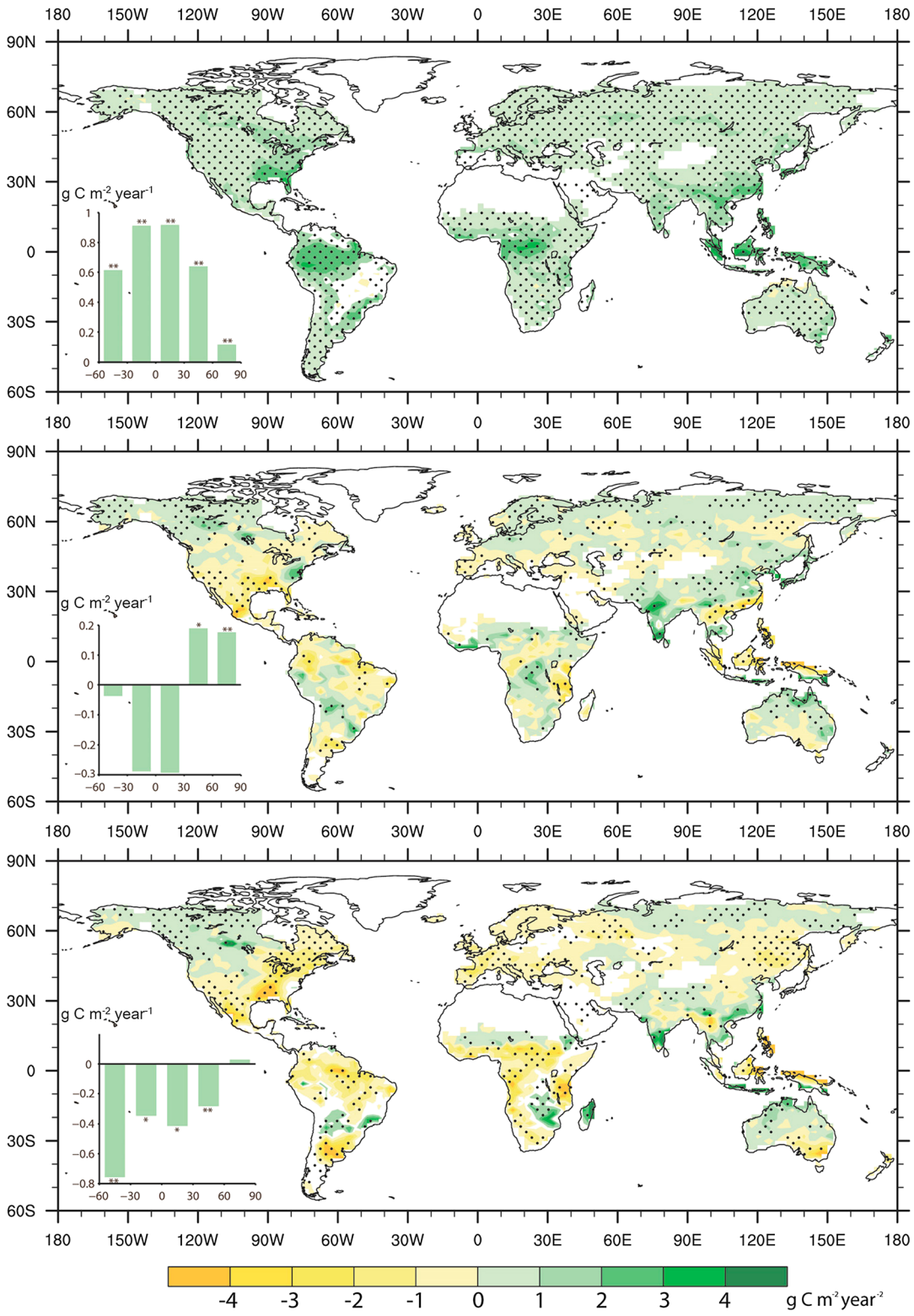

Figure 2. Global GPP (g C m^{-2}) change in response to CO_2 fertilization (FERT-OCTR), radiative forcing (RAD-CTR), and vegetation-climate feedback (VCF-FERT-CTR). GPP changes in response to climate change caused by (a) the fertilization effect of CO_2, (b) the radiative effect of CO_2, and (c) CO_2-induced vegetation-climate feedback over 1930–2011. Changes were analyzed with a linear regression model, and an *F* test was applied to test its significance. The dotted areas are regions where trends are statistically significant at the 90% level and all nonvegetated land areas are in grey. The insets in Figures 2a–2c show the mean GPP change (g C m^{-2}, vertical axis) from 60°S to 90°N at a 30° interval. The double asterisk means significance of the trends at the 99% level; the single asterisk means significance of the trends at the 95% level; no sign means not significant.

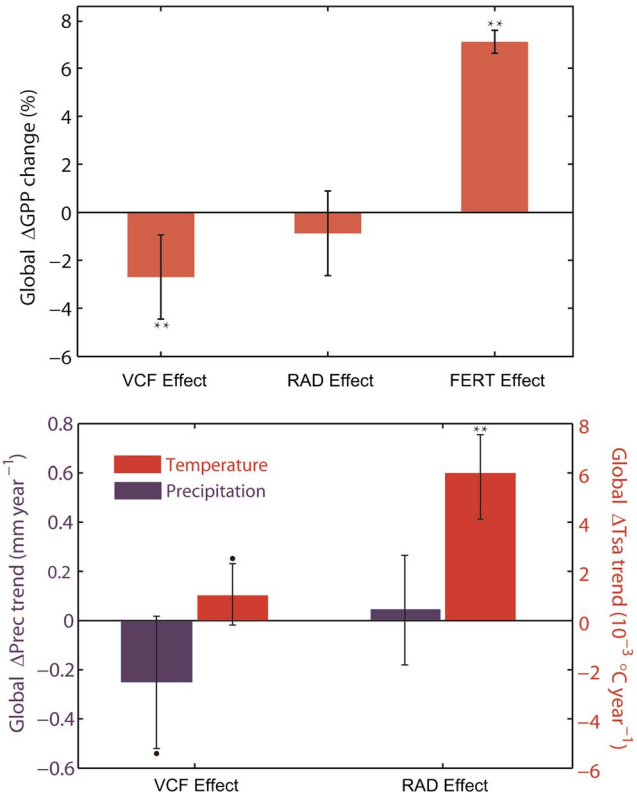

Figure 3. Global effect of CO_2 on ΔGPP, ΔPrec, and ΔTsa trend over 1930–2011. (a) Percentage of terrestrial GPP change in response to vegetation-climate feedback (VCF effect), CO_2 radiative climate change (RAD effect), and fertilization effect (FERT effect). (b)Terrestrial mean ΔPrec and ΔTsa in response to vegetation-climate feedback and CO_2 radiative climate change. Error bars indicate the 95% confidence interval of ΔPrec and ΔTsa trend. The double asterisk means significance of the trends at the 99% level; the bullet means significance of the trends at the 90% level; no sign means not significant.

Summing ΔGPP_{FERT}, ΔGPP_{RAD}, and ΔGPP_{VCF} gives a global net increase of global GPP, consistent with evidence from the Dole effect from oxygen isotopes of O_2 trapped in ice for preindustrial GPP [*Ciais et al*., 2011] and current data-driven estimates [*Beer et al*., 2010; *Zhao et al*., 2005] and from indirect deuterium isotopomer measurements on plant material [*Ehlers et al*., 2015]. Both the radiative and eCO_2-VCF have a net negative impact on global GPP, which jointly offsets approximate half of the fertilization-induced increase of GPP (Figure 3a). Climate change from eCO_2-VCF causes a larger global reduction of GPP ($-2.7 \pm 1.8\%$ over 1930–2011) than radiative climate change ($-0.9 \pm 1.8\%$ GPP change over 1930–2011). Given that the global ΔGPP_{FERT} is 8.9 ± 0.6 Gg C (equivalent to $9.4 \pm 0.64\%$ per 100 ppm) over the period of 1930–2011, vegetation-climate feedback offsets 38% of the eCO_2-FERT increase of GPP.

The effects of eCO_2-RAD and eCO_2-VCF on growing-season climate can be compared to each other. Growing-season surface air temperature differences due to radiative climate change (ΔTsa_{RAD}, detailed information is shown in Table S2) show a total increase of 0.49 ± 0.15 K ($p < 0.001$) over 1930–2011, close to the observed global warming magnitude [*Hansen et al*., 2010]. Slightly more land areas show positive precipitation change due to radiative climate change ($\Delta Prec_{RAD}$) (Figure 4d), resulting in nonsignificant positive global mean $\Delta Prec_{RAD}$. Global mean growing-season surface air temperature change due to eCO_2-VCF (ΔTsa_{VCF}) is a small warming of 0.081 ± 0.081 K ($p = 0.08$). The spatial pattern of ΔTsa_{VCF} showed growing-season warming over most of America and northern Eurasia, and less areas experienced cooling than warming (Figure 4a). This result is consistent with the results from *Shevliakova et al*. [2013]. Further analysis shows that stomatal regulated transpiration reduction is a larger relative signal of $7.7 \pm 1.5\%$ (Figure S3). Global mean precipitation changes in growing season due to eCO_2-VCF, $\Delta Prec_{VCF}$, is a net decrease of 21 ± 21 mm during 1930–2011 ($p = 0.07$) (Figure 3b). The spatial distribution of the global trend $\Delta Prec_{VCF}$ suggests that more areas are subject to decreasing precipitation (Figure 4c), especially the significant negative trend of $\Delta Prec_{VCF}$ in eastern North America, the Amazon basin, western Siberia, and northeast China, areas of high precipitation recycling through ET. When the global land areas are divided into humid and arid areas according to the soil water content threshold, arid areas where eCO_2-VCF result in an increase of precipitation experience more cooling compared to humid areas (Figures 4 and S5).

Because of the key role of transpiration in controlling the water vapor in the atmosphere over continents [*Trenberth et al*., 2009] and its recycling to land precipitation [*Van der Ent et al*., 2010]. Time series of global annual mean ΔET and ΔPrec changes by eCO_2-RAD (Figure S4a) and eCO_2-VCF (Figure S4b) were analyzed to explain the precipitation reduction. We found that there is a slight, nonsignificant increase in ET in

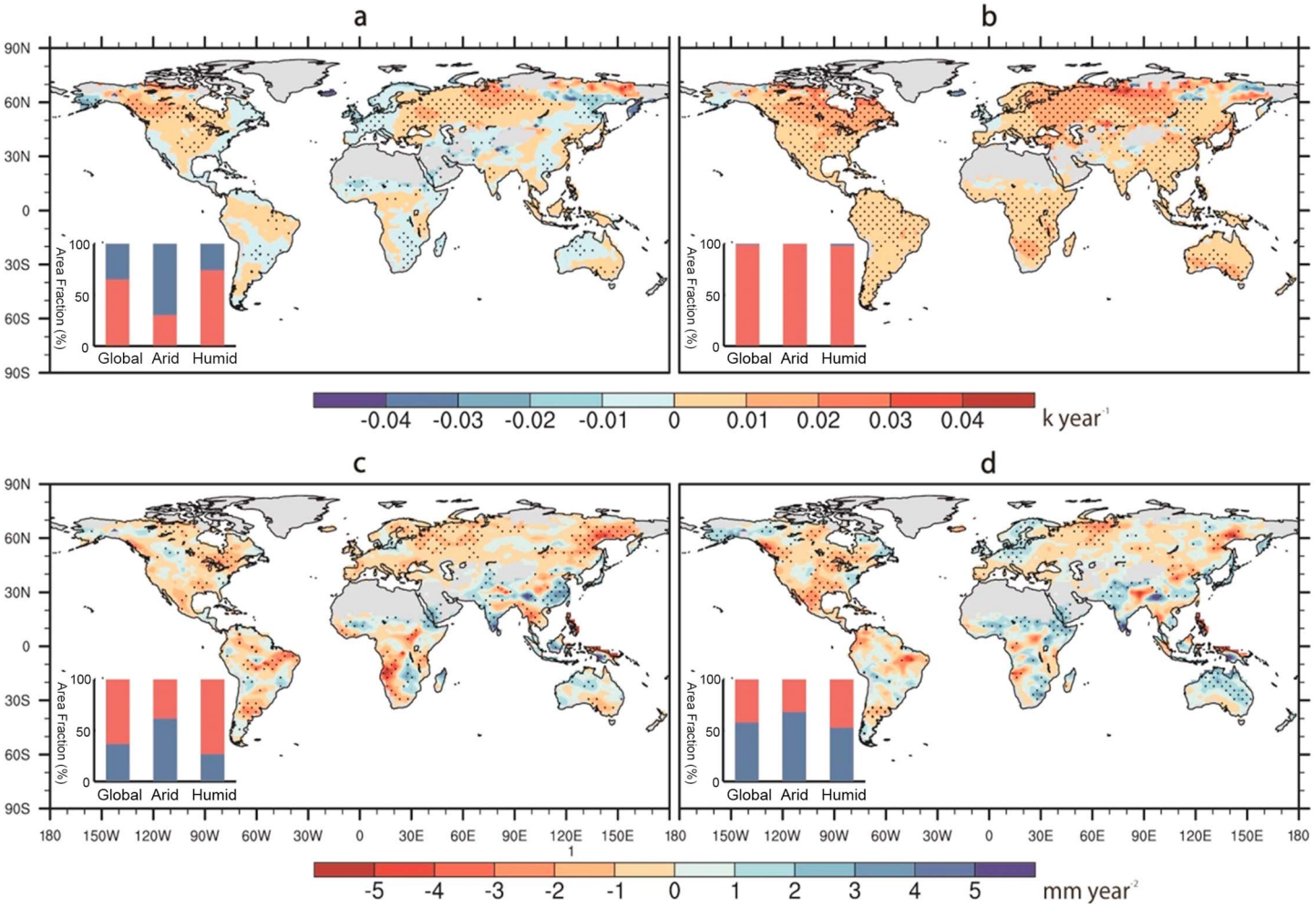

Figure 4. Global ΔTsa (K yr^{-1}) and ΔPrec (mm yr^{-2}) trend in response to elevated CO_2 between 1930 and 2011 in the CESM earth system model. Trend of global (a and b) ΔTsa (K yr^{-2}) and (c and d) ΔPrec (mm yr^{-2}) between 1930 and 2011 in response to CO_2 vegetation-climate feedback (Figures 4a and 4c) and CO_2 radiative climate change (Figures 4b and 4d) effects (in ΔPrec blue represents positive trend and red represents negative trend; in ΔTsa just the reverse). The dotted areas are regions where trends are statistically significant at 10% level using *F* test. The insets in Figures 4a–4d show the fraction of the land grids with positive and negative ΔPrec, ΔTsa trends in global, humid, and arid environments. Global areas are divided into humid and arid types according to the annual mean soil water content, where the soil water content above the 30% percentile is rated as humid areas, otherwise arid areas.

response to eCO_2-RAD and a significantly larger decrease in ET from eCO_2-VCF. Overall, in our coupled model, transpiration reduction due to eCO_2-VCF (13 ± 1.4% over 1930–2011) from stomatal closure at leaf scale is much higher than the increase of transpiration due to higher foliage cover (5.4 ± 0.9% over 1930–2011) (Figure S3). The spatial distribution of ΔET in CO_2-FERT experiment confirms the negative feedback of leaf area increase on the reduction in ET in arid area [*Andrews et al.*, 2011] (Figure S5) and thus on the cooling from eCO_2-VCF in water-limited area and warming in most other area (Figure 4a). Positive correlations are found between ΔET and ΔPrec over land ($R = 0.53$ under radiative climate change, $R = 0.61$ under eCO_2-VCF). This suggests that the decreasing $\Delta Prec_{VCF}$ is primarily caused by reduced ET.

Global land areas were divided into six biomes according to the dominant plant types used in the model to show the response of different biomes to rising atmospheric CO_2. All biomes except tundra show significant negative GPP change under vegetation-climate feedback (Figure S6) because in our model, most terrestrial ecosystems have water-limited GPP and vegetation-climate feedback causes a drying trend. The largest negative change in ΔGPP_{VCF} occurs in C3 grasslands. Significant positive ΔGPP_{rad} trends are found in tundra and boreal biomes, while ΔGPP_{RAD} across all other biomes shows a nonsignificant negative trend. This is very likely caused by continuous increase of extreme hot days in land [*Seneviratne et al.*, 2014] and drought-

induced stomatal closure due to enhanced vapor pressure deficit (VPD) and potential evapotranspiration [*Novick et al*., 2016], which is confirmed by the model result that 70% areas show increasing VPD in radiative climate change experiment (Figure S7). The ΔGPP_{FERT} is positive across all biomes, with the largest increases in temperate forests. Tropical forests and C3 grass is generally higher than the rate in boreal tree, tundra, and C4 grass. This is consistent with CO_2 fertilization being more effective in warm and arid area [*Norby et al*., 2005; *Smith et al*., 2000], while less in cold environment [*Hickler et al*., 2008] and insensitive for C4 vegetation [*Ehleringer et al*., 1997].

The output from IPSL-CM5A-LR is also analyzed here. It is noted that climate change from eCO_2-VCF and eCO_2-FERT effects jointly contribute to increase ΔGPP (total increase of 23.4 Pg C over 1850–2005), while the trend of ΔGPP due to eCO_2-RAD is nonsignificantly decreasing (-0.94 Pg C yr^{-1} over 1850–2005; Figure S9). Previous off-line simulations, the land surface model in IPSL-CM5A-LR, shows that the response of global GPP to rising atmospheric CO_2 alone (eCO_2-FERT) is 35 Pg C yr^{-1} per 100 ppm CO_2 (33 Pg C yr^{-1} over 1850–2005) [*Piao et al*., 2013]. Consequently, there is a 9.7 Pg C yr^{-1} difference between the two results, which implies that approximately 29% of the eCO2-FERT increase of GPP was offset by the negative effect of eCO_2-VCF in this coupled model. This result from the IPSL-CM5A-LR is comparable to the 38% reduction from eCO_2-VCF in CESM1.2.2, but the carbon model version of IPSL-CM5A-LR was not exactly the same than the one used to attribute eCO_2-FERT in the off-line experiment, which leads to more uncertainty in this result than for the set of CESM1.2.2-BGC experiments. The trend of climatic variables in IPSL-CM5-LR shows a similar pattern in CESM1.2.2-BGC, i.e., that eCO_2-VCF resulted in more areas experiencing precipitation decrease and warming, leading to a significant global decline in ΔPrec and increase in ΔTsa, while radiative climate change causes both global mean ΔTsa and ΔPrec to increase (Figures S10–S12 and Table S3). At the global scale, the correlation between ΔGPP and ΔPrec in IPSL-CM5A-LR were weaker than in CESM-BGC (Figure S14), whereas positive correlation between ΔGPP and ΔPrec and the negative correlation between ΔGPP and ΔTsa were consistent between the two models (Figures S8 and S14). These results from the IPSL-CM5A-LR thus confirm the negative impact of CO_2 climate forcing on terrestrial GPP, especially the significantly negative impact of vegetation-climate feedback on GPP.

4. Summary

Our results demonstrate that vegetation-climate feedback caused by rising CO_2 have significant contributions to GPP trends. Although CO_2 fertilization [*Norby et al*., 2005] and warming effects [*Matthews et al*., 2005; *Xia et al*., 2014] in driving global vegetation productivity have been previously addressed, our research further shows that warming due to CO_2 radiative climate change has no significant impact on the global GPP because of the spatially divergent responses of GPP to warming. In contrast, vegetation-climate feedback causes a significant reduction in global GPP mainly by reducing growing-season precipitation in 60°S–60°N latitude bands. On the other hand, a recent study suggested that semiarid ecosystems are important in regulating the interannual variation of GPP and net ecosystem exchanges due to an enhanced response to precipitation [*Poulter et al*., 2014]. Here our results imply that vegetation-climate feedback tends to bring more precipitation in dry areas through the positive precipitation-ET feedback by fertilization-caused increase in foliage cover [*Andrews et al*., 2011] while decrease precipitation in other areas. Given the important role of CO_2 in regulating terrestrial carbon cycling and the climate prediction uncertainties in response to increasing CO_2 [*Good et al*., 2015], more efforts are needed to reduce the uncertainty in climate-carbon feedback.

Acknowledgments
We thank Colin Prentice for the discussion and comments and the constructive reviews by Trevor Keenan. The model results of IPSL-CM5A-LR are downloaded from https://pcmdi.llnl.gov/projects/esgf-llnl/. This research is funded through projects to Q.Z. by NASA Land Use and Land Cover Change program (NASA-NNX09A126G) and NSF CDI Type II project (IIS-1028291). The model data underlying this research can be made available by contacting the corresponding authors.

References

Andrews, T., M. Doutriaux-Boucher, O. Boucher, and P. M. Forster (2011), A regional and global analysis of carbon dioxide physiological forcing and its impact on climate, *Clim. Dyn.*, *36*, 783–792, doi:10.1007/s00382-010-0742-1.

Arora, V. K., et al. (2013), Carbon-concentration and carbon-climate feedbacks in CMIP5 earth system models, *J. Clim.*, *26*, 5289–5314, doi:10.1175/JCLI-D-12-00494.1.

Ball, J. T., I. E. Woodrow, and J. A. Berry (1987), A model predicting stomatal conductance and its contribution to the control of photosynthesis under different environmental conditions, *Prog. Photosynth. Res.*, (953), 221–224, doi:10.1007/978-94-017-0519-6_48.

Beer, C., et al. (2010), Terrestrial gross carbon dioxide uptake: Global distribution and covariation with climate, *Science*, *329*(5993), 834–8, doi:10.1126/science.1184984.

Boucher, O., A. Jones, and R. A. Betts (2009), Climate response to the physiological impact of carbon dioxide on plants in the Met Office Unified Model HadCM3, *Clim. Dyn.*, *32*, 237–249, doi:10.1007/s00382-008-0459-6.

Cao, L., G. Bala, K. Caldeira, R. Nemani, and G. Ban-Weiss (2010), Importance of carbon dioxide physiological forcing to future climate change, *Proc. Natl. Acad. Sci.*, *107*, 9513–9518, doi:10.1073/pnas.0913000107.

Ciais, P., et al. (2011), Large inert carbon pool in the terrestrial biosphere during the Last Glacial Maximum, *Nat. Geosci.*, *5*, 74–79, doi:10.1038/ngeo1324.

Collatz, G. J., J. T. Ball, C. Grivet, and J. A. Berry (1991), Physiological and environmental regulation of stomatal conductance, photosynthesis and transpiration: A model that includes a laminar boundary layer, *Agric. For. Meteorol.*, *54*(2–4), 107–136, doi:10.1016/0168-1923(91)90002-8.

Cox, P. M., R. a. Betts, C. D. Jones, S. a. Spall, and I. J. Totterdell (2000), Acceleration of global warming due to carbon-cycle feedbacks in a coupled climate model, *Nature*, *408*(6809), 184–187, doi:10.1038/35041539.

Donohue, R. J., M. L. Roderick, T. R. McVicar, and G. D. Farquhar (2013), Impact of CO_2 fertilization on maximum foliage cover across the globe's warm, arid environments, *Geophys. Res. Lett.*, *40*, 3031–3035, doi:10.1002/grl.50563.

Ehleringer, J. R., T. E. Cerling, and B. R. Helliker (1997), C-4 photosynthesis, atmospheric CO_2 and climate, *Oecologia*, *112*(3), 285–299, doi:10.1007/s004420050311.

Ehlers, I., A. Augusti, T. R. Betson, M. B. Nilsson, J. D. Marshall, and J. Schleucher (2015), Detecting long-term metabolic shifts using isotopomers: CO_2-driven suppression of photorespiration in C3 plants over the 20th century, *Proc. Natl. Acad. Sci.*, (16), 1–6, doi:10.1073/pnas.1504493112.

Farquhar, G. D., S. von Caemmerer, and J. A. Berry (1980), A biochemical model of photosynthetic CO_2 assimilation in leaves of C3 species, *Planta*, *149*(1), 78–90, doi:10.1007/BF00386231.

Frank, D. C., et al. (2015), Water-use efficiency and transpiration across European forests during the Anthropocene, *Nat. Clim. Chang.*, *5*, 579–583, doi:10.1038/nclimate2614.

Friedlingstein, P., et al. (2006), Climate-carbon cycle feedback analysis: Results from the C4MIP model intercomparison, *J. Climate*, *19*, 3337–3353, doi:10.1175/JCLI3800.1.

Good, P., et al. (2015), Nonlinear regional warming with increasing CO_2 concentrations, *Nat. Clim. Chang.*, *5*(January), 138–142, doi:10.1038/nclimate2498.

Hansen, J., R. Ruedy, M. Sato, and K. Lo (2010), Global surface temperature change, *Rev. Geophys.*, *48*, RG4004, doi:10.1029/2010RG000345.1.

Hickler, T., B. Smith, I. C. Prentice, K. Mjöfors, P. Miller, A. Arneth, and M. T. Sykes (2008), CO_2 fertilization in temperate FACE experiments not representative of boreal and tropical forests, *Glob. Chang. Biol.*, *14*, 1531–1542, doi:10.1111/j.1365-2486.2008.01598.x.

Jung, M., et al. (2011), Global patterns of land-atmosphere fluxes of carbon dioxide, latent heat, and sensible heat derived from eddy covariance, satellite, and meteorological observations, *J. Geophys. Res.*, *116*, doi:10.1029/2010JG001566.

Matthews, H. D., A. J. Weaver, and K. J. Meissner (2005), Terrestrial carbon cycle dynamics under recent and future climate change, *J. Clim.*, *18*, 1609–1628, doi:10.1175/JCLI3359.1.

Matthews, H. D., M. Eby, T. Ewen, P. Friedlingstein, and B. J. Hawkins (2007), What determines the magnitude of carbon cycle-climate feedbacks?, *Global Biogeochem. Cycles*, *21*, GB2012, doi:10.1029/2006GB002733.

Medlyn, B. E., et al. (2015), Using ecosystem experiments to improve vegetation models, *Nat. Clim. Chang.*, *5*, 528–534, doi:10.1038/nclimate2621.

Melaas, E. K., A. D. Richardson, M. A. Friedl, D. Dragoni, C. M. Gough, M. Herbst, L. Montagnani, and E. Moors (2013), Using FLUXNET data to improve models of springtime vegetation activity onset in forest ecosystems, *Agric. For. Meteorol.*, *171–172*, 46–56, doi:10.1016/j.agrformet.2012.11.018.

Norby, R. J., et al. (2005), Forest response to elevated CO_2 is conserved across a broad range of productivity, *Proc. Natl. Acad. Sci.*, *102*, 18,052–18,056, doi:10.1073/pnas.0509478102.

Novick, K. A., et al. (2016), The increasing importance of atmospheric demand for ecosystem water and carbon fluxes, *Nat. Clim. Chang.*, *6*, 1023–1027, doi:10.1038/nclimate3114.

Piao, S., et al. (2013), Evaluation of terrestrial carbon cycle models for their response to climate variability and to CO_2 trends, *Glob. Chang. Biol.*, *19*, 2117–2132, doi:10.1111/gcb.12187.

Poulter, B., et al. (2014), Contribution of semi-arid ecosystems to interannual variability of the global carbon cycle, *Nature*, *509*, 600–603, doi:10.1038/nature13376.

Seneviratne, S. I., M. G. Donat, B. Mueller, and L. V. Alexander (2014), No pause in the increase of hot temperature extremes, *Nat. Clim. Chang.*, *4*, 161–163, doi:10.1038/nclimate2145.

Shevliakova, E., et al. (2013), Historical warming reduced due to enhanced land carbon uptake, *Proc. Natl. Acad. Sci.*, *110*, 16,730–16,735, doi:10.1073/pnas.1314047110.

Smith, S. D., et al. (2000), Elevated CO_2 increases productivity and invasive species success in an arid ecosystem, *Nature*, *408*(6808), 79–82, doi:10.1038/35040544.

Taylor, K. E., R. J. Stouffer, and G. A. Meehl (2012), An overview of CMIP5 and the experiment design, *Bull. Am. Meteorol. Soc.*, *93*, 485–498, doi:10.1175/BAMS-D-11-00094.1.

Trenberth, K. E., J. T. Fasullo, and J. Kiehl (2009), Earth's global energy budget, *Bull. Am. Meteorol. Soc.*, *90*, 311–323, doi:10.1175/2008BAMS2634.1.

Ukkola, A. M., I. C. Prentice, T. F. Keenan, A. I. J. M. van Dijk, N. R. Viney, R. B. Myneni, and J. Bi (2015), Reduced streamflow in water-stressed climates consistent with CO_2 effects on vegetation, *Nat. Clim. Chang.*, *6*, 75–78, doi:10.1038/nclimate2831.

Van der Ent, R. J., H. H. Savenije, B. Schaefli, and S. C. Steele-Dunne (2010), Origin and fate of atmospheric moisture over continents, *Water Resour. Res.*, *46*, W09525, doi:10.1029/2010WR009127.

van der Sleen, P., P. Groenendijk, M. Vlam, N. P. R. Anten, A. Boom, F. Bongers, T. L. Pons, G. Terburg, and P. A. Zuidema (2015), No growth stimulation of tropical trees by 150 years of CO_2 fertilization but water-use efficiency increased, *Nat. Geosci.*, *8*(January), 24–28, doi:10.1038/ngeo2313.

Xia, J., J. Chen, S. Piao, P. Ciais, Y. Luo, and S. Wan (2014), Terrestrial carbon cycle affected by non-uniform climate warming, *Nat. Geosci.*, *7*, 173–180, doi:10.1038/ngeo2093.

Zhao, M. S., F. A. Heinsch, R. R. Nemani, and S. W. Running (2005), Improvements of the MODIS terrestrial gross and net primary production global data set, *Remote Sens. Environ.*, *95*, 164–176, doi:10.1016/j.rse.2004.12.011.